Simulation of Pollen Transport by Wind: I. The Cellular Automaton Model

E Novotny [a] and J. Perdang [b]

[a] Scientists for Global Responsibility, Unit 2.8, Halton Mill, Mill Lane, Halton, Lancaster, Lancs., LA2 6ND, United Kingdom
E-mail: evan@sgr.org.uk
[b]Astrophysique Bât. B5, 17, Allée du Six Août, B-4000 Liège, Belgium

Summary. A Cellular Automaton (CA) model is developed to describe the creation, dispersal and deposition of pollen by low-altitude winds. Such models give a picture of pollen deposition and outcrossing patterns, as influenced by type and speed of wind, size of source field and other factors. Our aim is to illustrate how the general characteristics of pollen transport and deposition can be calculated, rather than to attempt to reproduce with precision the situation in any given farm or landscape. In principle, any degree of complications in the topography, wind conditions, soil roughness, etc. can be incorporated; it is only available memory and computing time that set limits.

The models require a number of input parameters that cannot be obtained directly from observations. Chief amongst these is the 'sticking' probability of the pollen, which can nevertheless be estimated by comparison of the results of our models with results obtained experimentally.

In this paper, we first consider the amount of deposited pollen as a function of distance from the source, comparing a particular set of observations obtained from a field experiment with the exponential decline often used to approximate such observations. We show that our models can provide a better fit to the field experiment than does the exponential decline, if the parameters of the modelling are suitably chosen. Our models can also produce decay curves showing humps, similar to those sometimes observed.

The concepts employed in the CA computer program are described, including both the computational procedures and the physical modelling. Extensions that may be incorporated into our present modelling, such as inclusion of higher-altitude winds and of topography of terrain, are also mentioned. Finally, we offer as a verification of the validity of our CA model the results of a numerical experiment exhibiting diffusion of pollen released from a single column of plants as the pollen progresses across a field.

It is left to Paper II to treat outcrossing and to show the diverse deposition patterns arising from various components of complex winds, and from other factors.

Key words: simulation, cellular automaton, pollen transport, pollen deposition, gene flow

1. Introduction

In this paper, we develop a computationally simple, parametrised cellular automaton (CA) model simulating pollen dispersal by the effect of wind.

Our simulation is based on a 2-dimensional CA framework as described in the literature [Perdang and Lejeune (1993)] and as specialised for hydrodynamic growth processes [Perdang (1996, 1999)]. Similar models have been devised for a variety of natural phenomena, including forest fires [Pandey (1991), Stauffer and Pandey (1992), Boccara *et al*. (1994), Seiden and Schulman (1990)]. Studies of pollen flow using different methods of modelling include those of Angevin *et al.* (2008), Geels *et al.* (2004), Gorelli *et al.* (2008) and Ushiyama *et al.* (2009).

Pollen is assumed to be produced in a prescribed spatial area of the model lattice; and its progress, from release by the parent plant, followed by travel on the wind and finally to deposition, is tracked for a succession of time-steps. In principle, a realistic simulation of the pattern and amount of pollen deposition or outcrossing, whether by this or any other method, would require a full knowledge of the detailed wind velocity (both magnitude and direction) over the entire area of the experiment at every instant of time corresponding to the duration represented in the simulation. Also required would be a minute knowledge of the quantity of pollen released by every individual pollen generator, and of the quantity of pollen captured by every individual pollen receptor, under the momentary weather conditions at every instant throughout the duration of the time represented (normally the several days of pollination). Clearly, it would not be practicable to aim for such a precise model. What can readily be achieved is to produce a model using typical values for parameters such as wind velocity. The probability of deposition ('sticking' probability) is the parameter in our method that would be most difficult to evaluate experimentally, and we therefore employ the technique of calibration often used in applications of physical theory to actual problems: this will be described in Paper II.

Extensions that may be incorporated into our present modelling, such as inclusion of higher-altitude winds and of topography of terrain, are mentioned. It is left to Paper II to treat outcrossing and to show the diverse deposition patterns arising from various components of complex winds, from the geometry of the source field and from other factors.

An underlying assumption of our scheme, as implemented here, is that the species whose pollen transport we are considering is anemophilous. This is essentially the case for maize, for example, although in the general case bees and other insects are also possible vectors of pollination [Bateman (1947), Percival (1955), Vaissière and Vinson (1994)]. More generally, dispersal of pollen by insects could be incorporated in CA modelling. The area of the deposit as evaluated in our model is then a minimum area.

The main purpose of this paper is to devise a detailed simulation model that enables us, in principle, to take account of realistic, non-stationary wind conditions and of the time-dependent supply of pollen from the source field. In this version of the model, however, we concentrate on Tauber's (1965, 1967) second component of pollen load in the air, namely, the

local pollen dispersed by down-wind and transported directly by a wind parallel to horizontal ground. The contribution of Tauber's (1965, 1967) regional pollen, at higher altitudes, is thereby not taken into account. As we shall mention below, however, our model lends itself to a straightforward extension that incorporates a computationally simple treatment of high-altitude winds, including upward convection and transport followed by deposition. However, this expansion into the third dimension requires much more computer memory. In all our CA modelling, only the pollen that remains within the limited spatial range of the simulation is tracked until it is deposited. If computer capacity suffices, the model can also be extended to include non-uniform topography and the presence of barriers, hedges or other obstacles, and other complicating factors.

2. Approximations to pollen deposition with distance.

2.1 The simple exponential approximation vs. *observations*

A typical decline with distance from the source field of the amount of pollen deposited, with subsequent seed production, is exhibited in Fig. 1. This plot shows the average percentage of outcrossed maize kernels as a function of distance *s* from the source field, measured in the direction of the wind; averages were taken over a period of 3 years (Jones and Brooks, 1950). In these experiments, a wide source plot of yellow maize was upwind from eight small plots of white maize placed in staggered fashion at various distances; these served as receptors for the pollen from the source plot. Although the data refer to numbers of cross-fertilised kernels rather than to the amount of deposited pollen, we assume that the relative numbers of the two varieties of these kernels are essentially the same as the relative amounts of the two varieties of deposited pollen at any location. We ignore the small effects of (1) capture of pollen from the source plot by the physical blocking by the receptor plots, (2) capture of pollen from the source plot by deposition within receptor plots upwind of a given plot and (3) contribution of receptor-type pollen from upwind receptor plots. Accordingly, we regard here the average Jones and Brooks data as first approximations to pollen deposition with distance. In the literature such a decay is called *negatively exponential* or *leptokurtic* [Raybould and Gray (1993)], suggesting that the decay actually obeys an exponential law.

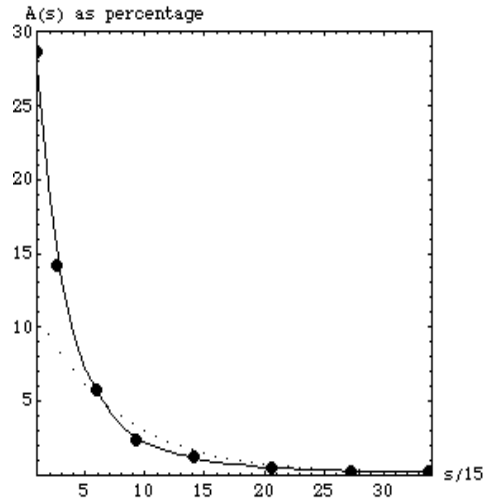

Fig.1. Percentage of outcrossing against distance *s* (in metres) from the edge of the source field. *Circles*: Data from Jones and Brooks (1950) Table 2. *Dotted curve:* best exponential fit. *Solid curve:* best fit obtained by Eq. (3), with n = 4.

Theoretically, an exponential law is expected to hold if the deposit of pollen conforms to a standard absorption phenomenon. The requirements to be satisfied are that the following factors must be constant (in time) and uniform (in space): (a) the pollen supply from the source field, (b) the wind and other weather conditions and (c) the absorptive properties of the recipient area. In this case, the amount of pollen, dA, deposited over a small interval of distance, ds, is proportional to ds and to the amount of pollen $A(s)$ available at distance s,

$$dA = - K A\, ds. \qquad (1)$$

The proportionality factor K (= $1/D$, where D is the decay length) is determined by the stationary weather conditions, in particular, the wind speed and presence or absence of rain, and by the properties of the recipient area. It may be interpreted as the probability of deposition of pollen per unit length.

To test the applicability of the underlying assumptions (a), (b), (c), we compare the observations with the best fit by the exponential curve solution to Eq. (1)

$$A(s) = A(0) \exp(-s/D),$$

where $A(s)$ is the amount of pollen deposited at distance s and $A(0)$ is the amount deposited at the edge of the source field. Fig. 1 displays the results of the comparison between the exponential approximation and the observations. At small distance from the source field, the observational curve has a slope that is steeper than the best-fit exponential decline, so that $A(0) = 14.5$ in the fit, against 28.6 for the observed value. On the other hand, the tail of the observed distribution decays more slowly than the best-fit exponential. The local decay length depends strongly on the distance, as is clear from the overall best-fit shown by the

solid curve (Eq. 2 with polynomial of degree n = 4). The exponential distribution is thus seen to be a poor approximation to the full set of observations. Consequently, the observational data rule out the validity of the assumptions of constancy and uniformity mentioned above. This conclusion is not surprising. Over the period of time of the transport of pollen the assumption of stationarity of the wind, in particular, is never satisfied; and likewise, in general, the weather conditions are not constant either. Moreover, space-independence of the wind over distances of the order of magnitude with which we are concerned is unusual.

At large distances (> 300 m), we find that the decline fits an approximate power law of exponent 2.5:

$$A(s)/A(0) \propto (1/s)^{2.5}.$$

Other attempts to represent the decline by simple analytical representations include those of Levin and Kerster (1974).

2.2 Polynomial approximation to exponent

Observed deposition curves may show irregularities while exhibiting a general decrease of deposit with distance. This behaviour can arise from variable weather conditions, irregularities in pollen production and non-uniform degrees of roughness or wetness across the recipient field during the time of pollination. It is clear that a simple exponential function cannot fit such complicated curves; and we describe next the introduction of polynomials into the exponent.

A straightforward generalisation of *ansatz* (1) with a constant coefficient K consists in regarding the latter as *space-dependent*. Expanding the space-dependence in a truncated power series

$$K(s) = K_o + K_1 s + K_2 s^2 + \ldots + K_{n-1} s^{n-1} + O(s^n), \qquad (2)$$

we have as the corresponding solution to Eq. (1):

$$A(s) = A(0) \exp[-P_n(s)], \qquad (3)$$

with $P_n(s)$ a polynomial of degree n in the distance s:

$$P_n(s) = K_o s + \tfrac{1}{2} K_1 s^2 + \ldots + 1/n \, K_{n-1} s^n.$$

Physically we may interpret the space-dependence (2) as reflecting a direct *space-dependence* of the physical conditions (wind, humidity, etc); but, in addition, the formal space-dependence (3) may also result indirectly from a *time-dependence* of the physical conditions (alternation of dry and humid weather, for instance).

2.2.1 Comparison with observations

Examples of experimental data exhibiting a rise or dip before the overall decline sets in are provided by Paterniani and Stort (1974) and by Jones and Brooks (1950) Table 3. That such behaviour could be real is supported by our models. In Fig. 2, the rate of pollen creation was time-dependent, as described in the caption. An approximate fit is achieved with an exponent containing a polynomial of degree 10. Fig. 3a illustrates an indirect time-dependence in the form of a change from wet to dry conditions, while Fig. 3b illustrates the combined time- and space-dependence of the wind and time-dependence of pollen creation. Both Fig. 3a and Fig. 3b can be approximated by Eqs. (2) and (3) with n = 8. In Fig. 1 we have also indicated that the averaged Jones and Brooks data can be fitted by Eq. (3) with n=4.

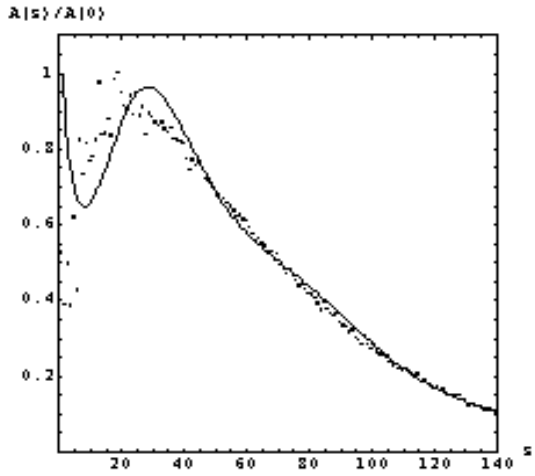

Fig. 2. Relative amounts of deposited pollen. CA model results (dots) for time-dependent probability of creation (P_c) proportional to $(t/T_c)(1 - t/T_c)$ for $0 \leq t < T_c$, and $P_c = 0$ for $t > T_c$, where T_c is time at end of creation of pollen. The continuous curve is the best fit with Eq. (3), with n = 10.

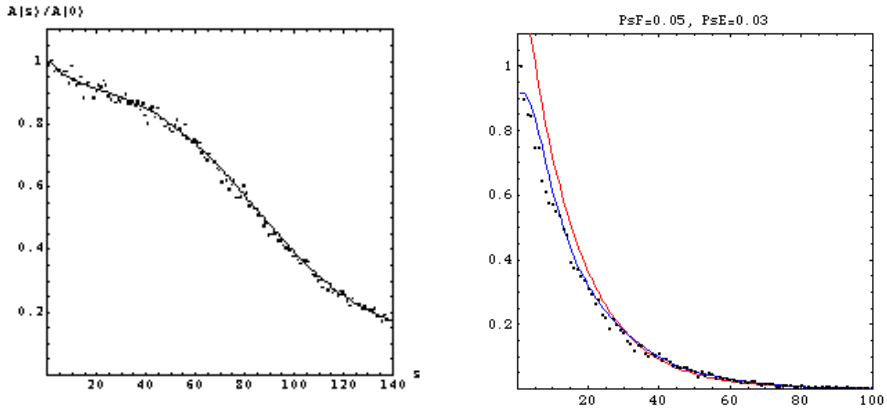

Fig. 3. Relative amounts of deposited pollen. (a) Left panel: Normalised pollen deposit in a simulation in which the probability of deposition changes from low initially (dry weather) to high (rainy weather); and pollen creation ends after a period t_c (dots). Corresponding fitting using Eqs. (2) and (3) with $n = 8$ (continuous curve). The break in the curve is the result of the change in the weather conditions. (b) Right panel: Pollen deposit under time- and space-dependence of the wind and time-dependence of pollen creation (which ends after a period T_c) (dots), and corresponding fitting using Eqs. (2) and (3) with $n = 8$ (blue curve). Although the simulation shows a leptokurtic distribution, the simple exponential fit (red curve) does not provide a good approximation.

3. The cellular automaton model

3.1 Description of the model and main parameters

Our models are based on a 2-dimensional CA framework, in which *space* (the total land area in which we are interested) is represented by a regular lattice of square cells, which are the smallest spatial units the model can resolve. Fig. 4 shows a lattice with only a small number of cells. The length Δs of a side of a cell defines the CA *unit of length*. The physical magnitude of Δs is a free parameter of the model; the typical range of values we have in mind is 10 to 50 metres. It is only after the computation is completed that a desired physical magnitude is assigned to Δs, to represent some particular application. In most of our numerical experiments we have adopted a rectangular lattice of 150×50 cells (with actual length of the lattice being 1.5 to 7.5 km). In some of our experiments the lattice has been increased to 300×80 cells (physical length 3 to 15 km). The donor field is usually chosen as a square area of 20×20 cells (200 m to 1 km). Functions of position within the lattice will be designated with arguments (x,y), where x and y are the integer CA co-ordinates, as defined in Fig. 4.

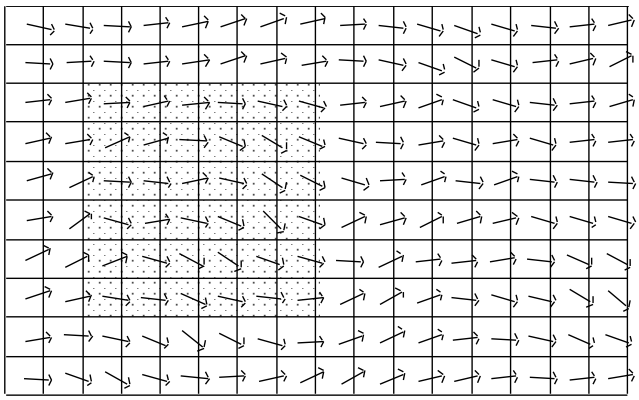

Fig. 4.- Lattice universe showing the geometry, location and orientation of the donor field (dotted area). The arrows in each cell (x,y) indicate an instantaneous wind direction $\boldsymbol{v}(x,y)$ at a given time (averaged over the cell). Positive x is to the right, positive y is upwards. The origin is at the lower left corner of the lattice.

Time is discrete and is measured by an integer $t = 0,1,2,\ldots, T_{\text{exp}}$, counting the number of time steps that have elapsed since the moment of first release of pollen; T_{exp} is the (finite) number of steps over which the actual numerical calculation is performed. The duration of one time-step, Δt, defines the CA *unit of time*. Like the CA unit of length, this magnitude is a free parameter of the model and is assigned a dimensional value only after the computation has been completed. The order of magnitude of Δt must be chosen so that the wind can carry the pollen no farther than the neighbouring cell during one time-step. Let us denote the maximum wind speed by v_{M} and the maximum speed of the pollen by v_{MP}. Then, if the cell size, Δs, is given, the time-step is required to obey

$$\Delta t \;\leq\; \Delta s / v_{\text{MP}}$$

For a medium-strength wind (v_{M} = 5 to 10 m/s, which is 18 to 36 km/hr), with v_{MP} equal to v_{M}, and with a cell-size Δs = 50 m, we have a time-step Δt = 10 to 5 seconds. Under the action of the wind, pollen may flow from a cell to one of its four nearest neighbours along the directions of positive x or y, or along negative x or y. Motion along a diagonal to the grid is possible only as a zig-zag during successive time-steps. Whether or not motion takes place, and in which direction, is determined probabilistically, as will be explained later.

In our model, pollen is allowed to exist in 3 *states* or forms in a given cell, namely, (a) as *releasable pollen* (if the cell is in a source field); (b) as *air-borne pollen*; and (c) as *deposited pollen*. The amounts of each form of pollen in a given cell at a time-step t are denoted by $A_{\text{c}}(t)$ (where the subscript c stands for 'created and releasable'), $A_{\text{f}}(t)$ (where f stands for 'free and air-borne') and $A_{\text{s}}(t)$ (where s stands for 'sticking and deposited'), respectively. In discussing the simple models of this paper, we shall use the term 'created' to mean 'created and releasable' (if the wind is strong enough) and we shall use 'sticking' to be synonymous with 'sticking and deposited'. A situation could arise in which pollen temporarily sticks but

becomes air-borne again, and hence is not ‘deposited’. However, we avoid this complication in the present models.

Amounts of pollen are measured in a CA unit Δa, which is again a parameter of the model; it is assigned a physical magnitude only in a physical application. This unit is chosen such that a field cell contains, on average, a total amount of the order of 10-100 units of *releasable* pollen (which becomes actually *released* pollen over the whole period of pollination). For example, the average maize plant produces 14 to 50 x 10^6 pollen grains over the period of pollination, which is typically 5 to 8 days or, more rarely, 2-14 days (Purseglove, 1972; Miller, 1985). If we assume that each plant occupies an area of 0.3 m^2, then a cell of size 50 m contains 8000 plants, or about 1 to 4 x 10^{11} pollen grains; convenient orders of magnitude of Δa are then 10^{10} or 10^{11} grains.

The amounts per cell of the different pollen forms change according to the following *processes*. (a) The amount of air-borne pollen in a given field cell increases by the *release* of pollen in that field cell: $\Delta A_c \rightarrow \Delta A_f$, where the arrow means ‘changes state to’; (b) the amount of air-borne pollen increases by *inflow* from an adjacent cell: $\Delta A_f' \rightarrow \Delta A_f$; (c) the amount of air-borne pollen decreases by *outflow* to a neighbouring cell: $\Delta A_f \rightarrow \Delta A_f''$; and (d) the amount of air-borne pollen decreases by *deposition* of air-borne pollen: $\Delta A_f \rightarrow \Delta A_s$.

Table 1 summarises the quantities used in the CA model.

Table 1. Main model parameters. The second column gives the dimensional scaling factor. Δs, Δt and Δa serve as our units of length, of time and of amount of pollen in the CA model. For example, if the wind velocity in a particular cell and at a particular time-step is v (a pure number, say 0.1), then, in a particular application, if Δs is assigned the value 50 m and Δt is assigned the value 10 sec, the wind velocity is v $\Delta s/\Delta t$ = 0.5 m/sec in that cell at that time-step.

V	$\Delta s / \Delta t$	total wind-speed
W	$\Delta s/\Delta t$	uniform wind component
v	$\Delta s/\Delta t$	critical wind-speed below which no pollen can be carried off
f_V	1	entrainment factor (fraction of local wind-speed with which pollen is carried
T	Δt	total duration of a run
T	Δt	total time interval over which all pollen is released (single or multiple spasmodic event)
N	$\Delta a\, \Delta s$	total amount of pollen creatable, per cell-area
P	Δt	probability of release of pollen per cell-area and per time-step
P	Δt	probability of deposition and sticking of pollen per cell-area of region external to source field, per time-step
P	Δt	probability of deposition and sticking of pollen per cell-area of source (donor field), per time-step

We now discuss our simulation of these processes in some detail.

3.2 Treatment of pollen creation and release

The pollen-release process (a), in the words of Treu and Emberlin (2000), occurs 'spasmodically' or on a 'diurnal basis'. We describe this release in a field cell stochastically, in terms of a time-dependent transition probability, $P_c(t)$. The latter, which is the probability per time-step of creation and release of one unit of pollen, Δa, at time-step t in one cell, is an empirically given input function for the model. This probability is also a function of (x,y); but, for lack of experimental data, we assume it to be constant over an entire area occupied by a particular crop. For the purposes of the simulation we represent $P_c(t)$ by a multi-parameter continuous function $f(t;T_P)$, with the property that it vanishes outside the time interval $[0,T_P]$ over which pollination is taking place. The simple representation we have adopted in most of our numerical experiments is the following:

$$f(t;T_P) = P_o\,(1 - t/T_P)(t/T_P) \quad \text{if} \quad 0 \le t \le T_P; \qquad (4)$$
$$f(t;T_P) = 0 \quad \text{if} \quad t < 0 \ \text{ or } \ t > T_P,$$

which is applicable to a *single spasmodic event* in which pollen suddenly begins to be released from plants all over the field. The parameter T_P should be a few thousand time-steps (for example, with a time-step of 10 s and an event of 5 hours, T_P = 1800 time-steps). To reduce the amount of calculation, we have set T_P = 200 or 300 in most of our experiments. The coefficient P_o is a normalisation constant of the probability (see below).

Staggered release from different cells can also be modelled, but we have not programmed this at present.

In addition, the models could be made more realistic by introducing a probability function $P_c(t)$ that obeys a *cyclic* behaviour $\gamma(t/T_C)$, of cycle T_C corresponding to the time-scale of the individual spasmodic events (or to 24 h in the diurnal case). The overall period of pollination T_P (corresponding to 2 to 14 days) can be much larger than T_C; the cyclic behaviour then modulates a continuous function of type (4):

$$P_c(t) = \gamma(t/T_C)\, f(t;T_P).$$

In some trial experiments, we have adopted a cyclic function of the form

$$\gamma(t/T_C) = 1 + \cos\,[2\pi\,(t/T_C)]. \qquad (5)$$

In this case, the expression for the probability of creation is

$$P_c(t) = \{1 + \cos\,[2\pi\,(t/T_C)]\}\ (1 - t/T_P)(t/T_P).$$

A representation that would approximate reality yet more closely would regard the cyclic contribution (5) itself as a stochastic function, in which different cycles have different lengths and amplitudes.

We denote by $N\Delta a$ the maximum number of pollen grains available in one cell over the duration of the pollen release. The total amount of pollen released over the period of pollination by one field cell then becomes $N\Delta a \int dt\, P_c(t)$. Under the assumption that all of the available pollen is actually released, the integral, to be carried out over $[0,T_P]$, yields 1. The total amount $N\Delta$a must be determined empirically for the particular plants growing in the field and for the spacings between them. (For a typical maize field $N\Delta$a is of order of 10^{11} grains, for cells of size Δs = 50 m.)

3.3 Stochastic pollen transport. Simulation of the low-altitude wind

Pollen inflow to a cell (process (b)) and outflow from a cell (process (c)) is achieved by the action of wind. The wind pattern is ideally an empirically known input function of the

model. In our treatment we simulate this pattern as follows. We distinguish four wind contributions: (i) a time- and space-independent component, w, in the x-direction (along the length of the rectangular lattice); (ii) a wavelike propagating component, of zero average over space and time; (iii) a component localised in space and time; and (iv) a randomly fluctuating component of zero average. Contributions (ii) and (iv) simulate the non-steady and turbulent wind components, respectively, while effect (iii) describes a gust of wind.

Since pollen is typically expected to travel with a speed less than the actual local wind speed $v(x,y)$, we introduce an entrainment factor f_v (≤ 1), so that the propagation speed of the pollen becomes $V(x,y) = f_v v(x,y)$. The factor f_v is an input parameter that is independent of space and time in our model.

The actual transport of the air-borne pollen is treated stochastically as follows. Suppose, for instance, that the wind-velocity components v_x and v_y in cell (x,y) are both positive. Then the direction into which a pollen unit of the cell is moved is $(x+1,y)$ or $(x,y+1)$, with probability $v_x^2/(v_x^2 + v_y^2)$ or $v_y^2/(v_x^2 + v_y^2)$, respectively. Suppose the direction chosen is $(x+1,y)$. Then each unit amount of pollen Δa is individually shifted to cell $(x+1,y)$ with probability proportional to the propagation speed $f_v v(x,y)$; or, alternatively, it remains in cell (x,y) with probability proportional to $(1-f_v)v(x,y)$. The decisions are achieved with a Monte Carlo method. The procedure guarantees that, *on average*, all the pollen in the cell (x,y) travels with a speed $f_v v(x,y)$. In addition, the probabilistic treatment generates a *diffusion* of the pollen around the average propagation. The diffusion effect will be discussed in connection with our numerical experiments.

As a further wind-related effect, our model incorporates the requirement that a cell (x,y) of the source field be allowed to release pollen only if the wind speed in that cell, $v(x,y)$, exceeds a threshold value v_c (again an empirical model parameter that is independent of space and time).

3.4 Stochastic pollen deposition

Process (d) of pollen deposition is described by a stochastic procedure similar to our treatment of pollen release. Ideally the model requires as an input a space- and time-dependent probability distribution, $P_S(x,y,t)$, which is the probability per unit time-step that an air-borne unit amount of pollen in cell (x,y) be deposited in the same cell at time-step t. We shall refer to this as a *deposition probability* or *sticking probability*. Physically the air-borne pollen is deposited via gravity onto the ground or, as a result of collisions, onto obstacles, including plants in the donor and recipient fields. The efficiency of these mechanisms depends on the wind and other weather conditions, on the nature and state of the soil and plants (in particular, humidity and roughness), and on vegetation and other barriers [Chamberlain and Chadwick (1972); Dupont (1985)]. It is reported, for instance, that the adherence efficiency of pollen on a wet surface is 3 to 10 times greater than on a dry surface.

In our simulation we allow for a time dependence in the probability function $P_S(x,y,t)$ of the form $P_S(x,y,t) = P_{So}(x,y)\,\varphi(t)$, where $\varphi(t)$ is an empirical function which enables us to take

account of the effect of time-dependent weather conditions. In most of our exploratory experiments we have set this modulating function equal to 1 (an exception is shown in Fig. 3a). Space dependence is reduced to a minimum by assuming that both the donor field and the outside zone are homogeneous. In our model the process of deposition is then described by

$$P_{so}(x,y) = P_{sF} \quad \text{if } (x,y) \text{ is a cell of the donor field;} \qquad (6)$$
$$= P_{sE} \quad \text{if } (x,y) \text{ is a cell exterior to the donor field,}$$

where the parameters P_{sF} and P_{sE} are the (constant) sticking probabilities inside and outside the donor field, respectively. The numerical values of these parameters must be adjusted to the observational data.

In the formulation in terms of a general function $P_s(x,y,t)$, the topographic contributions to pollen deposition must be included. For instance, the presence of a barrier essentially increases the local sticking probability. In the context of the simplified formulation (6), the influence of a barrier is described by an extra component:

$$P_s(x,y,t) = P_{sB} \quad \text{if } (x,y) \text{ is a cell of the barrier.} \qquad (7)$$

The parameter P_{sB} is the sticking probability inside the cells that simulate the barrier. In a more realistic treatment the surface topography, and in particular a barrier, modifies the wind profile as well (Raynor *et al*., 1974). This latter effect requires the introduction of additional parameters in the description of the wind. We mention that we have carried out some trial experiments in which a linear barrier (a row of cells normal to the wind direction) is simulated by the sticking effect (7). These experiments show that a high probability can efficiently block the propagation of pollen. In our systematic numerical experiments this effect is not included since we have tried to keep the number of free parameters minimal.

3.5 Treatment of high-altitude winds: three-dimensional extension of the model

As already pointed out, the model as formulated so far deals with the transport properties of a wind near the ground only. A formal transport of pollen by a high-altitude wind can be incorporated without unduly complicating the simulation procedure, as we describe below.

Besides the three states of pollen, we include a fourth form (d), *high-altitude pollen*, which is spread by winds at altitudes above approximately 500 m. The detailed dynamical treatment of the high-altitude pollen requires the full specification of the wind pattern in the higher layer (an input of our model). As in the case of the transport near the ground, we have processes of inflow and outflow that conform to the same rules as for the low-altitude wind. Creation and depletion of high-altitude pollen, A_h, are processes that merely transfer air-borne pollen from low altitude to high altitude, $\Delta A_f \rightarrow \Delta A_h$, and back from high altitude to low altitude, $\Delta A_h \rightarrow \Delta A_f$. These mechanisms are described by transformation probabilities per time-step and per cell, P_{fh} and P_{hf}, respectively, which are extra input parameters (or, more generally, input functions).

With the inclusion of the high-altitude wind component, three-dimensionality is implicitly incorporated in our model. A cell is now referred to by three integer CA co-ordinates, (x,y,z), where the third co-ordinate z labels the vertical layers. In principle, the wind in each cell is described by three velocity components, $v_x(x,y,z)$, $v_y(x,y,z)$, $v_z(x,y,z)$. In its simplest form, the model is considered to comprise three layers in the vertical direction. The first layer ($z = 1$) simulates the 'ground', which may be the actual ground or vegetation (including plants in the donor and recipient fields) or possibly low barriers, or some combination of these. The state of a cell of this layer describes the amounts of pollen created and deposited; there is no wind associated with the ground layer. The second layer ($z = 2$) simulates the atmosphere near the ground. The state of a cell of this layer specifies the low-altitude wind velocity and the amount of pollen in suspension in this wind. The third layer ($z = 3$) mimics the high altitudes. The state of a cell of that layer is specified by the high-altitude wind velocity and the amount of free pollen carried by the high-altitude wind.

If detailed empirical data on the 3-dimensional wind-velocity field and local pollen density are available, then this scheme of layering can be made arbitrarily fine, by choosing a large number n of layers labelled $z = 1, 2, \ldots, n$.

Once the pollen is released (in level $z = 1$), it is carried away by the low-altitude wind (layer $z = 2$); or, possibly, it might be immediately deposited (level $z = 1$). In this picture, a cell in any given layer $1 < z < n$ can gain pollen from, or lose pollen to, a cell immediately above, $(z+1)$, or below it, $(z-1)$, as well as from or to any neighbouring cell in the same layer. Exchange of pollen between layers is engineered by the action of a vertical component of the wind velocity.

In the simplified 3-layer model the vertical velocity component is ignored ($v_z(x,y,z) = 0$), its role being played by exchange probabilities. The probability function $P_{fh}(x,y,2,t)$ for upward motion generates a pollen-flux component from layer $z = 2$ to layer $z = 3$, while the probability function $P_{hf}(x,y,3,t)$ corresponds to a downward flux from $z = 3$ to $z = 2$. In the case of a high barrier extending to level $z = 3$, deposition can be treated by assigning a probability $P_{hg}(x,y,b,3)$ to the cells $(x,y,3)$ of the barrier .

In the two-dimensional model, we had implicitly what we now, in the three-dimensional case, regard as two layers: in layer $z = 1$, pollen is created and also deposited; in layer $z = 2$, pollen is carried by horizontal motion. In the three-dimensional picture we have, in addition, vertical motion in both directions between adjacent layers, such as layers $z = 2$ and $z = 3$ (schematically treated in terms of probabilities of exchange). What we referred to as transformations among different states of pollen in the two-dimensional interpretation of our model now presents itself as vertical motions of a single kind of pollen in this three-dimensional picture. For example, the deposition of pollen in a ground cell, $z = 1$, (described by the probability function $P_s(x,y,t)$ of the two-dimensional model) is actually a pollen inflow from a cell of layer $z = 2$ to its neighbouring cell in layer $z = 1$. The vertical downward pollen flux from cell $(x,y,2)$ to cell $(x,y,1)$ is, in the two-dimensional model, $A_f(x,y,t)\, P_s(x,y,t)\, \Delta a$, with $A_f(x,y,t)$ the amount of airborne pollen in cell (x,y) at step t.

4. Application to propagation exhibiting diffusion

4.1 Results from the model

We have carried out an exploratory experiment that serves not only to pinpoint the special effects of the probabilistic treatment of pollen transport but also to demonstrate the validity of our CA modelling.

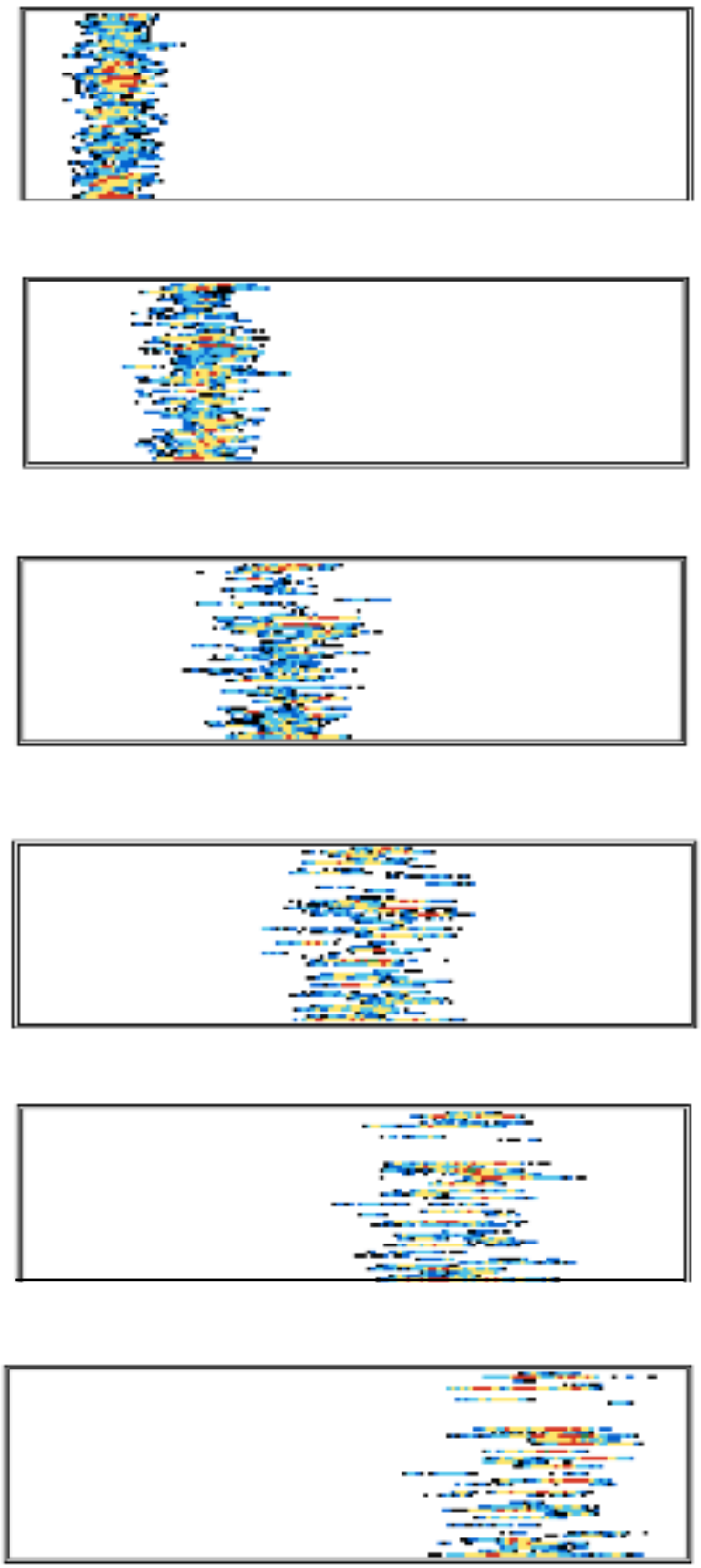

Fig. 5.- Propagation of an initially thin line of pollen as it is carried by wind, in successive frames, from left to right at equal intervals between 100 and 600 time-steps.

For particular choices of the parametrisation, the model formalism is reducible to a partial differential equation that admits of an analytic solution. The latter can be compared with the numerical simulation. We begin with analysing one of the simplest integrable cases, that of the spreading thin line of pollen. We shall consider spreading in the x-direction only.

Consider a donor field that contains a single row of plants, simulated on our standard CA lattice by one column of cells at CA co-ordinates $x = x_f = 1$, $y = 1, 2, \ldots, 50$. Suppose further that the pollen is released instantaneously, at time-step $t = 0$, and that the deposition probabilities can be neglected ($P_S(x,y,t) = 0$). Accordingly, once the pollen is released, it remains air-borne over the duration of the experiment, for $t = 1, 2, \ldots, T_{exp}$. Finally, assume that the wind is uniform over this period of time and has a dimensionless speed $w = 1$ in the positive x-direction. The pollen transport conforms to the process we have outlined in section 3.3 on *Stochastic pollen transport*; at any time step t, a unit amount of pollen propagates either with maximum speed 1 (and with probability f_V) or with speed 0 (and probability $1-f_V$). The resulting average speed of motion is then $f_V w$. This very schematic model necessarily implements fluctuations in the propagation speed. The results indeed illustrate the expected gradual spreading of an initially thin line of pollen as it is carried gently down-wind. Fig. 5 shows the effect at equal intervals between 100 and 600 timesteps.

The numerical results as given by our CA model are summarised in Fig. 6, using parameter values $N = 100$, $f_V = 0.2$, $T_{exp} = 600$. The successive curves illustrate the distribution over the CA lattice of the amount of air-borne pollen at different time-steps. The vertical strip originally (at $t = 0$) of width equal to the cell size Δs propagates down-wind with the average uniform speed of 0.2. Simultaneously, the width of the air-borne pollen distribution is seen to increase. The Figure exhibits the spatial pollen profile $Q(s,t)$ as a function of distance s from the donor field (*i.e.*, from the column of cells at $x = x_f$), at the times $t = 100, 200, \ldots, 600$. The numerical value of $Q(s,t)$ is the total amount of pollen in the column of cells at position $x = x_f + s$ at time-step t; the quantity $Q(0,0)$ represents the total available quantity of pollen in the field, which is released at time 0. At any later time-step t the profile $Q(s,t)$ is seen to be well approximated by a Gaussian propagating with speed 0.2. The height of the Gaussian is decreasing while the width is increasing with time. In our scheme, this change in height and width in the pollen profile is linked to the discreteness of the local speed (0 or 1 in dimensionless form) of the individual unit amounts of pollen in the CA treatment, which requires a probabilistic approach (if f_V is not 0 or 1). The spreading effect is therefore computationally inevitable. But in the context of natural transport problems, this *a priori* spurious model feature does correspond to a realistic physical effect. It mimics an ever-present irregular small-scale velocity component of the carrier wind (on a scale less than the spatial resolution Δs of the model) and necessarily induces fluctuations in the velocities of the individual 'fluid particles' (the unit amounts of pollen). Therefore, these 'particles' carry out random walks in the forward direction. The decaying Gaussian profile is precisely the fingerprint of this diffusion process.

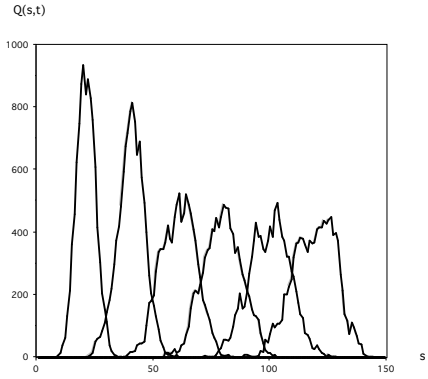

Fig. 6.- Propagation of pollen by a uniform wind

4.2 Comparison with solution of a partial differential equation

We now show that this particular model can be recast into the form of a partial differential equation. The latter describes the evolution of the amount of pollen, $G(S,T)$, which is the quantity $Q(s,t)$ introduced above but now expressed in continuous variables (a single continuous space variable $S = s\,\Delta s$ and a continuous time $T = t\,\Delta t$, for a small-enough cell-size Δs and a small-enough time-step Δt). In fact, the balance equation for the amount of pollen $Q(s,t)$ can be written as follows:

$$Q(s,t) = (1 - f_v)\, Q(s,t\text{-}1) \; + \; f_v\, Q(s\text{-}1,t\text{-}1)$$

The first contribution on the right-hand side is the fraction $(1 - f_v)$ of the amount of pollen $Q(s,t\text{-}1)$ that was present in the column of cells at position s at the previous time-step, t-1, and that remains in the same row of cells at the current step t. The second contribution is the gain of pollen due to inflow from the neighbouring cell at s-1. Introduce now the continuous function $G(S,T)$, and expand $G(S+\eta,T+\varepsilon)$ with respect to the increments η and ε in a power series, keeping only the first-order terms in the time increment but both the first- and second-order terms in the spatial increment.[1] This leads to the following partial differential equation;

$$\partial/\partial T\, G(S,T) + v_{\text{trans}}\, \partial/\partial S\, G(S,T) = \; D \;\; \partial^2/\partial S^2\, G(S,T). \qquad (8)$$

[1] An equation with a second-order derivative in time and a first-order derivative in space would have resulted if we had kept the $O(\varepsilon)$ and $O(\varepsilon^2)$, and the $O(\eta)$ terms. However, in our transport problem the second–order time derivative ($O(\varepsilon^2)$ contribution) is not expected to become large in the course of the evolution. On the other hand, the spatial curvature ($O(\eta^2)$ contribution) is always large near the peak of the distribution. Hence, the physically relevant expansion for this problem is given by Eq. (8). It should be kept in mind that the highest-order term in a Taylor expansion is not accurately represented. Hence the analytical expression of the coefficient D (Eq. 9) is not expected to be very accurate either; D should rather be regarded as an adjustable parameter.

The two macroscopic parameters v_{trans} (macroscopic dimensional velocity) and D (dimensional diffusion coefficient) are related to the CA parameters by the following expressions:

$$v_{trans} = f_v \, \Delta s/\Delta t$$

$$D = \delta \Delta s^2/\Delta t \; = 1/2 \, f_v \, \Delta s^2/\Delta t \; = 1/2 \, v_{trans} \, \Delta s. \qquad (9)$$

The coefficient δ plays the part of a dimensionless diffusion constant.

Eq. (8) has the following particular solution:

$$G(S,T) \; = \; K \;\; T^{-1/2} \;\; \exp \, [\, - \, (S - v_{trans} \, T)^2/(4 \, D \, T) \,]. \qquad (10)$$

If we let the continuous time T tend to zero, then $G(S,T)$ tends to a delta-function concentrated at $S = 0$. But at time $T = 0$ the actual pollen distribution in the formal limit of our donor field shrinking to a line-segment (one column of cells whose size tends to zero) is precisely given by a delta peak. The free constant K in relation (10) is then a measure of the total amount of pollen available in the field.

As can be judged from an inspection of Fig. 6, the pattern (10) is duplicated by the CA result, within the limits of the statistical fluctuations and the resolution of the discrete model. This can be seen by examining, as functions of time, the position of the maximum of the distribution [$S_{max}(T)$ or $s_{max}(t)$], and the variance, which we denote by $\sigma(T)^2$ or $\Sigma(t)^2$. From Eq. (10) we have the theoretical relations

$$S_{max}(T) \; = v_{trans} \, T \qquad \text{and} \qquad \sigma(T)^2 \; = \; 2 \, D \, T. \qquad (11)$$

The numerical values of $s_{max}(t)$ and $\Sigma \, (t)^2$ are found, for given t, by fitting a Gaussian profile to the computed CA distributions. Fig. 7 (left frame) shows that the dimensionless distance of the peak measured from the edge of the field, $s_{max}(t)$, indeed increases linearly with time t. A least-squares fit of the numerical results of the CA calculation gives the relation

$$s_{max}(t) \; = \; 2.30 + 0.194 \, t,$$

with a slope differing from the theoretical slope ($f_v = 0.20$) by 3%. The presence of the extra term 2.30 is a consequence of fitting a line $y = a + m \, x$ to the results of the CA experiment. The deviation from zero of this extra term is an indicator of the precision of the small-scale CA model for solving the partial differential equation (or *vice versa*). When we fit a line $y = m \, x$, then we obtain $m = 0.192$ ($= f_v$), a slope that differs only slightly from the previous estimate.

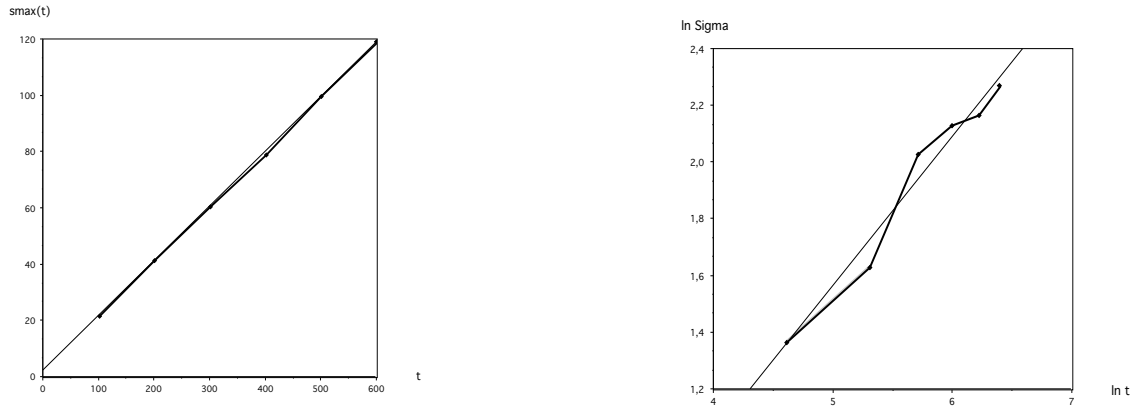

Fig. 7.- Experimental s_{max} *vs* t and $\ln\Sigma$ *vs* $\ln t$ relations (dots) compared with the theoretical relations (straight lines).

The dimensionless counterpart of the second of Eqs. (11) may be written as

$$\Sigma(t)^2 = 2\,\delta\,t. \qquad (12)$$

From Fig. 7 (right frame) it also transpires that the logarithm of $\Sigma(t)$ increases linearly with the logarithm of the time-step. The least-squares fit gives

$$\ln \Sigma(t) \;=\; -\,1.07 \;+\; 0.527 \ln t.$$

This expression may be compared with that obtained from the theoretical relation, Eq. (12). If we eliminate δ in Eq. (12) by using Eq. (9), we have

$$\begin{aligned} \ln \Sigma(t) &= 1/2\;\ln f_V \;+\; 1/2\;\ln t \\ &= -\,0.805 \;+\; 0.500 \ln t. \end{aligned} \qquad (13)$$

The CA experiment duplicates the theoretical slope 1/2 in Eq. (13), characteristic of a diffusion phenomenon, with a precision of 5%. The dimensionless diffusion constant measured from the widths of the peaks of Fig. 6 is $\delta = 0.06$. As expected, this value is rather different from the 'theoretical' estimate (Eq. 9), $\delta = 1/2\,f_V = 0.10$, although it remains of the right order of magnitude.

The numerical experiment we have described is indicative that when a differential representation for a CA behaviour exists, then even a small-sized CA (150×50 cells) can reproduce it with reasonable accuracy. This behaviour is properly duplicated even over relatively short time-intervals, although formally the equivalence of both representations is shown to hold for $t \rightarrow \infty$ only. Perhaps more importantly this implies that differential models (such as the diffusion-type equation discussed by McCartney (1994)) can then be solved, and generalised, via an associated CA model. The latter has the advantage that complicated mechanisms, such as space- and time-dependent pollen deposition, which are not easy to implement in a differential formulation, are trivially dealt with in a CA model.

5. Discussion

The cellular automaton model provides a straight-forward and transparent technique for describing and predicting the flow of pollen as driven by wind. We have shown explicitly how pollen creation, transfer by wind and deposition can be treated. Input parameters in our models include the probabilities, as functions of time, of (i) creation and release of pollen (considered to be simultaneous) and (ii) sticking (considered to be the same as deposition). Also required are (iii) an entrainment factor, which accounts for the possibility that the pollen does not travel with the full speed of the wind; and (iv) a minimum wind-speed needed to carry off the pollen from the plant. In addition, (v) the temporal and spatial dependence of the wind velocity must be specified over the lattice.

Our numerical experiments have not included high-altitude winds, but the actual model does incorporate a schematic treatment of the effects of these winds. Although not included in the present work, extension of the model to distribution of pollen by insects could be added. In fact, this modelling technique lends itself well to the inclusion of many complicating factors, such as the presence of barriers, each of which can be applied as an add-on module.

6. Conclusions

The cellular automaton model provides a simple and convenient way to simulate the dispersal of wind-borne pollen. The degree of complexity of which it is capable is limited only by the availability of observational data to fix the input parameters and by the capacity of the computer on which the program is run.

Our simulations show the steep declines in pollen deposition with distance from the source field that are observed in field experiments and which are sometimes approximated by exponential functions. The CA models can produce a better fit to observations than does a simple exponential function. Our models can also be made to exhibit the irregular declines sometimes observed.

We illustrate the gradual diffusion of pollen from plants growing in a single column of lattice cells, as the pollen is blown across the land by a uniform breeze.

In Paper II, we shall present results for various sets of values of some of the parameters and make further comparisons with observations.

Acknowledgments

We are grateful to the National Pollen Research Unit at University College Worcester for providing us with copies of some of the reference papers. We thank the Institute of Astronomy, Cambridge, for use of the premises during most of this work.

References

Angevin, F., Klein, E.K., Choimet, C., Gauffreteau, A., Lavigne, C., Messéan, A., Meynard, J.M., 2008. Modelling impacts of cropping systems and climate on maize cross-pollination in agricultural landscapes: The MAPOD model. Eur. J. Agron. 28, issue 3, 471-484. http://www.sciencedirect.com/science/article/pii/S1161030107001244

Bateman, A.J., 1947. Contamination in seed crops 2: Wind pollination. Heredity 1, 235-246.

Boccara, N., Cheong, K., Oram, M., 1994. A probabilistic automata network epidemic model with births and deaths exhibiting cyclic behaviour. J. Phys. A27, 1585-1597.

Chamberlain, A.C., Chadwick, R.C., 1972. Deposition of spores and other particles on vegetation and soil. Ann. Appl. Biol. 71, 141-158.

Dupont, L.M., 1985. Temperature and rainfall variation in a raised bog ecosystem. Rev. Palaeobot. Palynol. 48, 71-159.

Geels, C., Løfstrøm, P., Frohn, L.M., Brandt, J., Kjellsson, G., 2004. Wind dispersal of genetically modified pollen from oilseed rape and rye fields. Danish Research Centre for Organic Farming, No. 2.
DARCOFenews http://www.darcof.dk/enews/june04/pollen.html

Gorelli, S., Santucci, A., Balducci, E., Mazzoncini, M., Russu, R., 2008. Spatial simulation model to analyse pollen dispersal and coexistence scenarios between GM and GM-free crops, in: Breckling, B., Reuter, H., Verhoeven, R., (Eds.) 2008. Implications of GM Crop Cultivation at Large Spatial Scales, Theorie in der Ökologie 14, Frankfurt, Peter Lang.

Jones, M.D., Brooks, J.S., 1950. Effectiveness of Distance and Border Rows in Preventing Outcrossing in Corn. Oklahoma Agric. Experimental Station, Tech. Bull. No. T- 38.

Levin, D.A., Kerster, H.W., 1974. Gene flow in seed plants. Evol. Biol 7, 139- 200.

McCartney, H.A., 1994. Dispersal of spores and pollen from crops. Grana 33, 76-80.

Miller, P.D., 1985. Maize Pollen: Collection and Enzymology, in: Sheridan, W.F., (Ed.), Maize for Biological Research, Special publication of Plant Molec. Biol. Assoc., USA, pp. 279-282.

Novotny, E., Perdang, J., Paper II, Simulation of Pollen Transport by Wind: II. Numerical Experiments and Comparisons with Observations, http://www.sgr.org.uk/sites/sgr.org.uk/files/PollenTransport-Paper%20II-final-SGR.pdf

Pandey, R.B., 1991. Cellular automata approach to interacting cellular network models for the dynamics of cell population in an early HIV infection. Physica A 179, 442-470.

Paterniani, E., Stort, A.C., 1974. Effective maize pollen dispersal in the field. Euphytica 23, 129-134.

Percival, M.S., 1955. The presentation of pollen in certain angiosperms and its collection by *Apis mellifera.* New Phytologist 54, 353-36.

Perdang, J., 1996. Cloudy, filamentary and knotty structures: Simulating diffusive growth dynamics. Knowledge Transfer 1, 8-15.

Perdang, J., 1999. Cellular automaton explosion model, in: Leach, P.G.L., Bouquet, S.E., Rouet, J.L., (Eds.). Dynamical Systems, Plasmas, and Gravitation. Conferences and Schools in Physics 518, 210-226, Springer, Heidelberg.

Perdang, J.M., Lejeune, A., (Eds.), 1993. Cellular Automata: Prospects of Astrophysical Applications. World Scientific, Singapore.

Purseglove, J.W., 1972. Tropical Crops. Monocotyledons 1, Longman Group, London.

Raybould, A.F., Gray, A.J., 1993. Genetically modified crops and hybridisation with wild relatives: a UK perspective. J. Appl. Ecol. 30, 199-219.

Raynor, G.S., Ogden, E.C., Hayes, J.V., 1974. Enhancement of particle concentrations downwind of vegetative barriers. Agric. Meteorol. 13, 181-188.

Seiden, P.E., Schulman, L.S., 1990. Percolation model of galactic structure. Adv in Phys 39, 1-54.

Stauffer, D., Pandey, R.B., 1992. Immunologically Motivated Simulations of Cellular Automata. Computers in Phys 6, 404-410.

Tauber, H., 1965. Differential pollen dispersion and the interpretation of pollen diagrams. Dan. Geol. Unders. 2 rk 89.

Tauber, H., 1967. Investigations of the mode of transfer of pollen I: Forested areas. Rev. Palaeobot. Palynol. 3, 277-286.

Treu, R., Emberlin, J., 2000. Report for the Soil Association from the National Pollen Research Unit, University College Worcester.

Ushiyama, T., Du, M., Inoue, S., Shibaike, H., Yonemura, S., Kawashima, S., Amano, K., 2009. Three-dimensional prediction of maize pollen dispersal and cross-pollination, and the effects of windbreaks. Environ. Biosafety Res. 8, issue 4, 183-202.

Vaissière, B., Vinson, S.B., 1994. Pollen morphology and its effect on pollen collection by honey bees *Apis mellifera* L., with special reference to upland cotton*, Gossypium hirstum* L. Grana 33, 128-138.